



# Low temperature synthesis of $LnOF$ rare-earth oxyfluorides through reaction of the oxides with PTFE

S.E. Dutton\*, D. Hirai, R.J. Cava

Department of Chemistry, Princeton University, Princeton, NJ 08544, USA

## ARTICLE INFO

### Article history:

Received 7 November 2011

Accepted 9 December 2011

Available online 17 December 2011

### Keywords:

- A. Inorganic compounds
- B. Chemical synthesis
- C. X-ray diffraction
- D. Crystal structure
- D. Magnetic properties

## ABSTRACT

A low temperature solid-state synthesis route, employing polytetrafluoroethylene (PTFE) and the rare-earth oxides, for the formation of the  $LnOF$  rare-earth oxyfluorides ( $Ln = Y, La, Pr, Nd, Sm, Eu, Gd, Tb, Dy, Ho, Er$ ), is reported. With the exception of  $LaOF$ , which forms in a tetragonal variant, rhombohedral  $LnOF$  is found to be the major product of the reaction. In the case of  $PrOF$ , a transition from the rhombohedral to the cubic fluorite phase is observed on heating in air to 500 °C. X-ray diffraction shows the expected lanthanide contraction in the lattice parameters and bond lengths. Magnetic susceptibility measurements show antiferromagnetic-like ordering in  $TbOF$ ,  $T_m = 10$  K, with a metamagnetic transition at a field  $\mu_0 H_t = 1.8$  T at 2 K. An antiferromagnetic transition,  $T_N = 4$  K, is observed in  $GdOF$ . Paramagnetic behavior is observed above 2 K in  $PrOF$ ,  $NdOF$ ,  $DyOF$ ,  $HoOF$  and  $ErOF$ . The magnetic susceptibility of  $EuOF$  is characteristic of Van Vleck paramagnetism.

© 2011 Elsevier Ltd. All rights reserved.

## 1. Introduction

The  $Ln^{3+}$  cations have generated much interest due to their unique luminescent properties and potential applications in lasers [1,2], phosphors [3], and biological markers [4]. In phosphors some of the most successful host lattices are rare-earth oxyfluorides,  $LnOF$ , which have been extensively studied [5–7]. Current work on these compounds involves using new synthetic routes to control the shape and size of the nanoparticles to manipulate the fluorescence [8–14]. The luminescence of  $Ln^{3+}$  materials arises due to crystal electric field (CEF) effects in the  $4f$  orbitals. These same  $4f$  orbitals are responsible for the magnetism in  $Ln^{3+}$  containing materials. Rare-earth magnetism is of particular interest in the pyrochlore system [15–18] where, at low temperature, the frustrated lattice has been shown to exhibit both spin-ice [15–17] and spin-liquid [18] behavior. In the  $Ln^{3+}$  pyrochlores, the non-magnetic cations and oxygen displacement have a significant effect on the properties observed [17,18]. In rhombohedral  $LnOF$  the  $Ln^{3+}$  lattice is a distorted array of face-sharing  $Ln^{3+}$  tetrahedra that can be considered as a three-dimensional analogue of the highly geometrically frustrated edge-sharing triangular planar lattice. The low temperature magnetism of  $LnOF$  may thus be of interest. Only the magnetic susceptibility of  $NdOF$  has been previously reported [19,20]. However, given the sensitivity of the magnetism of the  $Ln^{3+}$  cations to changes in the crystal structure, the behavior may differ significantly across the  $LnOF$ s.

Typically rare-earth oxyfluorides,  $LnOF$ , have been made using a high temperature solid-state synthesis from the sesquioxides,  $Ln_2O_3$ , and rare-earth fluorides,  $LnF_3$  [21,22]. Ceramic synthesis of  $LnOF$  has also been carried out by reacting  $Ln_2O_3$  and a small excess of ammonium fluoride,  $NH_4F$ , at  $T \sim 900$  °C [19,20,23,24]. Other routes to  $LnOF$ s include using a sol-gel method [10,11] or precipitation from solvents [9,14]. Mechanochemical synthesis of  $LnOF$  has also been reported [12], and thin films have been made using chemical vapour deposition (CVD) [8,13]. Critically these routes focus on formation of the high temperature fluorite phase rather than the low temperature rhombohedral one. In this paper we report a method for the formation of  $LnOF$  at low temperatures. By using stoichiometric amounts of polytetrafluoroethylene (PTFE),  $CF_2$ , as the fluorination agent,  $LnOF$  can be formed from  $Ln_2O_3$  by a simple solid-state reaction. The reaction temperature,  $T \leq 650$  °C, allows for isolation of the low temperature rhombohedral phase. By tuning the reaction temperature we demonstrate that this simple method allows for the synthesis of the majority of the rare-earth oxyfluorides. From magnetic measurements we demonstrate that  $TbOF$  has an antiferromagnetic-like ordering transition at  $T_m = 10$  K with a metamagnetic transition observed at  $\mu_0 H_t = 1.8$  T at 2 K. We also show antiferromagnetic (AFM) ordering in  $GdOF$ ,  $T_N = 4$  K. In the other  $LnOF$  studied no magnetic ordering is observed for  $T > 2$  K, although the magnetic susceptibility of  $EuOF$  is characteristic of Van Vleck paramagnetism.

## 2. Experimental

Rare-earth oxyfluorides were synthesized using a solid-state reaction from their oxides and PTFE powder ( $CF_2$ ). Stoichiometric

\* Corresponding author. Tel.: +1 609 258 5556; fax: +1 609 258 6746.  
E-mail address: [sdutton@princeton.edu](mailto:sdutton@princeton.edu) (S.E. Dutton).

**Table 1**

Reaction conditions and lattice parameters for  $LnOF$ , obtained from X-ray diffraction measurements at room temperature. Phases have rhombohedral symmetry ( $R\bar{3}m$ ) except where noted.

$Ln$	Synthesis temp. ( $^{\circ}C$ )	Color	$a$ ( $\text{\AA}$ )	$c$ ( $\text{\AA}$ )	Impurity phases	Particle size (nm)	
Y	500	White	3.79528 (5)	18.8631 (3)	2.12 (10)wt% $Y_2O_3$	70 (7)	
La	500	White	4.0516 (2)	20.177 (3)	Tetragonal LaOF main phase 92 (2)wt%	31 (7)	
Pr	400	Cream	Cubic phase, $Fm\bar{3}m$ , $a = 5.66828$ (14) $\text{\AA}$			56 (11)	
Pr	1000	White	Cubic phase, $Fm\bar{3}m$ , $a = 5.66847$ (14) $\text{\AA}$			98 (3)	
Nd	500	Blue	3.9528 (2)	19.6995 (10)		29 (4)	
Sm	550	White	$Sm_4O_7F_6$ impurity phase, structure not known, no quantitative analysis				
Eu	500	White	3.88286 (8)	19.3274 (5)		103 (13)	
Gd	500	White	3.86469 (11)	19.2516 (7)		85 (11)	
Tb	400	Tan	3.83959 (12)	19.1134 (7)	3.0 (3)wt% $Tb_2O_3$	55 (4)	
Tb	1000	White	3.83966 (8)	19.1158 (5)	2.4 (2)wt% $Tb_2O_3$	101 (15)	
Dy	600	White	3.82052 (9)	18.9988 (5)		66 (9)	
Ho	650	Pink	3.80085 (6)	18.9000 (4)		90 (10)	
Er	500	Pink	3.78125 (7)	18.8075 (4)		34 (2)	

amounts of the sesquioxide,  $Ln_2O_3$  ( $Ln = Y, La, Nd, Sm, Eu, Gd, Tb, Dy, Ho, Er$ ), and PTFE were intimately mixed and pressed into pellets. In the case of PrOF and TbOF mixed valence  $Pr_6O_{11}$  and  $Tb_4O_7$  were used as starting materials rather than the corresponding  $Ln_2O_3$ . The lighter  $Ln_2O_3$  ( $Ln = La, Nd, Sm, Eu, Gd$ ) and  $Pr_6O_{11}$  oxides were pre-dried at  $800^{\circ}C$  prior to reaction. The pellets were sealed into evacuated quartz tubes and heated for 24 h. The exact temperature of the reaction depended on  $Ln$  and is detailed in Table 1. To remove the residual carbon present after heating, samples were heated in air at  $500^{\circ}C$  for 2 h. To ensure complete reduction of  $Ln^{4+}$ , samples of TbOF and PrOF were then heated in an evacuated quartz tube for 2 h at  $1030^{\circ}C$ .

Data for quantitative analysis of the crystal structures were collected over the angular range  $5 \leq 2\theta \leq 90^{\circ}$  with a step size of  $2\theta = 0.02^{\circ}$ , using a Bruker D8 Focus X-ray diffractometer operating with Cu  $K\alpha$  radiation and a graphite diffracted beam monochromator. Rietveld analysis [25] was carried out using the FULLPROF suite of programs [26]. Backgrounds were fit using a linear interpolation of data points and then fixed. The peak shape was modeled using a pseudo-Voigt function. Peak broadening was modeled using a symmetry dependent Scherrer analysis [27]. This phenomenological model employs a spherical harmonic expansion consistent with the Laue class of the crystals [28,29]. The size of the crystals can then be inferred by comparing the peak widths with those of a crystalline alumina standard.

Magnetization measurements on selected samples of  $LnOF$  were made on a Quantum Design Physical Properties Measuring System (PPMS). Magnetic susceptibility,  $\chi = M/H$ , measurements were made after cooling in zero field (ZFC) in a 1 T measuring field  $2 \leq T \leq 300$  K; for all but TbOF,  $M$  was linearly proportional to  $H$ ,  $\mu_0 H \leq 1$  T, in the measured temperature range. Due to the presence of a field-induced transition at low temperatures in TbOF, ZFC and field cooled (FC) magnetic susceptibility measurements were also made in a 0.1 T measuring field. Additionally, isothermal magnetization measurements,  $-9 \leq \mu_0 H \leq 9$  T, were carried out on TbOF, at selected temperatures, after cooling to the measuring temperature in a 0 T field using a Quantum Design PPMS.

### 3. Results and discussion

For all of the rare-earth oxyfluoride syntheses, formation of  $LnOF$  was observed, and even for YbOF and LuOF, not discussed here, significant quantities of  $LnOF$  were observed in addition to unreacted  $Ln_2O_3$ . Only the reaction of  $CeO_2$  with PTFE resulted in the formation of a lanthanide fluoride,  $LnF_3$ . The exact temperature of the reaction is highly dependent on the  $Ln$  element present. Beyond the relative ease with which mixed valence  $Pr_6O_{11}$  and

$Tb_4O_7$  were reduced to  $LnOF$ , there is no apparent trend in the temperature of formation of  $LnOF$  in the reaction with PTFE.

In all cases, the product was found to be black after the initial heating. Since  $LnOF$  is expected to have a pale color or be white, this dark shade is ascribed as due to residual carbon. On heating to  $500^{\circ}C$  in air a color change was observed for all of the  $LnOF$ . With the exception of PrOF, no significant changes were observed in the X-ray diffraction patterns. On heating PrOF to  $500^{\circ}C$  in air, a phase transition from the rhombohedral [30]  $R\bar{3}m$  phase to the cubic [31]  $Fm\bar{3}m$  fluorite structure was observed. The structures of the two phases are shown in the inset of Fig. 1. In both, the  $Ln^{3+}$  cations are cubically coordinated, with the cubes sharing edges to form a three

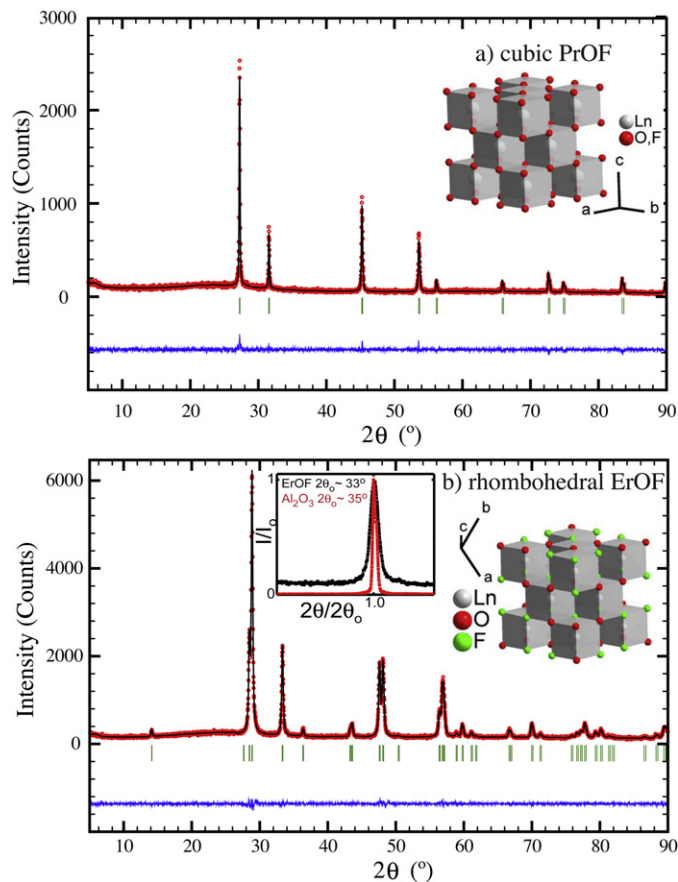


**Fig. 1.** X-ray diffraction for (a) cubic PrOF and (b) rhombohedral ErOF. The difference curve is also shown; reflection positions are indicated by the vertical lines. The structures for (a) cubic and (b) rhombohedral  $LnOF$  are inset. A comparison of the peak width in X-ray diffraction of ErOF and the  $Al_2O_3$  standard is also inset in panel (b).

dimensional array. The cubic phase of PrOF has the fluorite structure in which the  $O^{2-}$  and  $F^-$  anions are randomly distributed across the anion sites rather than forming the ordered layers observed in the rhombohedral phase. The cation ordering in the rhombohedral structure is accompanied by a small distortion from the ideal cubic fluorite lattice [22]. This structural transition has been observed at high temperatures in other LnOF [21]. When the temperature of the second firing step was reduced to 400 °C for PrOF, a mixture of both the high and low temperature phases was observed. Further reduction in the temperature of the second firing did not remove the residual carbon. In previous studies, the temperature of transition from the rhombohedral to the cubic structure in PrOF has been reported to be at ~800 °C [21–23]. This value is similar to that reported for other LnOF systems [21–23]. The anomalously low temperature of the transition to the fluorite phase in the current study may be facilitated by the presence of carbon or  $Pr^{4+}$ ; alternatively it could be a result of the instability of the fluorite phase for the larger  $Ln^{3+}$  cations. The latter is supported by the fact that tetragonal LaOF as the major phase in our synthesis of the La variant. Like rhombohedral LnOF, this phase has an ordered anion array but in the absence of a structural distortion has the tetragonal  $P4/nmm$  space group.

Following removal of the residual carbon, samples of TbOF had a dark tan color that suggested incomplete reduction of  $Tb^{4+}$ . This was confirmed by the change in color to white on heating to 1030 °C. Although a dramatic increase in the particle size was observed, no significant changes to the crystal structure were seen following this additional heating (Table 1). On heating to 1030 °C a less dramatic color change is also observed in PrOF; the cubic phase of PrOF is maintained although an increase in the particle size is observed after the additional heating. For simplicity, only the structure and properties of fully reduced PrOF and TbOF will be discussed below.

A quantitative structural analysis of the rhombohedral LnOF formed was carried out based on powder X-ray diffraction data, and is detailed in Tables 1 and 2. For cases where the structure of

rhombohedral LnOF was not previously reported, the structure of the closest LnOF was used for a starting point and the lattice parameters taken from the literature [22,24]. In the case of SmOF the presence of a  $Sm_4O_3F_6$  impurity phase [22] with an unknown structure was observed and thus, due to significant overlap between peaks from the two phases, a quantitative analysis of the SmOF structure was not attempted. Due to the relatively small contribution of the anions to the X-ray diffraction pattern, the isotropic temperature factor,  $B_{iso}$ , for the anion sites had no significant effect on the refinement and  $B_{iso}$  for both sites was therefore fixed at the arbitrary value of 0.7 Å<sup>2</sup>. The expected lanthanide contraction is observed in the size of the unit cell for rhombohedral LnOF (Fig. 2). Consideration of the Ln–Ln distances also indicates the expected lanthanide contraction (Fig. 2). Some deviations from the expected behavior are observed in the Ln–O and Ln–F bonds, this is most likely due to the large error in refinement of the position of the lighter  $O^{2-}$  and  $F^-$  ions using X-ray diffraction, rather than the result of deviations from the anticipated trend. In all cases significant broadening of the diffraction peaks is observed. This is due to the small particle size of the LnOF product and is a consequence of the low temperature of the reaction. A significant range in the size of the LnOF particles is observed, from 103 nm in EuOF to 29 nm in NdOF. From our experiments it appears that the LnOF phases are relatively stable, and thus it might be possible to tune the size of the particles using either the reaction temperature or a post formation anneal step for greater control of the particle size. For example, in NdOF a size range from 29 to 86 nm particles can be produced depending on the exact reaction conditions; the larger particles form in reactions with PTFE at 800 °C.

The magnetic susceptibility of selected samples of LnOF (Ln = Pr, Nd, Gd, Eu, Dy, Ho, Er) is shown in Fig. 3. In the case of PrOF, NdOF, DyOF, HoOF and ErOF the expected paramagnetic behavior is observed above 2 K. EuOF is also paramagnetic but due to low lying excited states has a temperature dependent susceptibility characteristic of Van Vleck paramagnetism. The behavior of the

**Table 2**  
Atomic positions and selected bond lengths for rhombohedral LnOF obtained from room temperature X-ray diffraction.

Ln	Ln 6c 00z		O 6c 00z <sup>a</sup>	F 6c 00z <sup>a</sup>	$R_{wp}$	$\chi^2$	Ln–Ln	Ln–O	Ln–F
	z	$B_{iso}$ (Å <sup>2</sup> )	z	z					
Y	0.7418 5 (6)	2.00 (5)	0.6211 (4)	0.8685 (3)	14.9	1.18	3.79528 (4) × 6 3.5842 (13) × 3 4.0882 (14) × 3	2.278 (8) 2.261 (2) × 3	2.389 (6) 2.435 (3) × 3
Nd	0.74221 (12)	0.82 (6)	0.6217 (13)	0.8697 (11)	25.8	1.23	3.9282 (12) × 6 3.751 (3) × 3 4.254 (3) × 3	2.37 (2) 2.360 (6) × 3	2.51 (2) 2.524 (9) × 3
Eu	0.74224 (11)	0.04 (6)	0.6199 (11)	0.8700 (10)	20.6	1.06	3.88286 (6) × 6 3.682 (2) × 3 4.174 (2) × 3	2.36 (2) 2.310 (5) × 3	2.471 (19) 2.475 (8) × 3
Gd	0.74205 (16)	0.10 (8)	0.6198 (15)	0.8704 (14)	26.1	1.05	3.86469 (8) × 6 3.661 (4) × 3 4.163 (4) × 3	2.35 (3) 2.298 (7) × 3	2.47 (2) 2.463 (11) × 3
Tb	0.74195 (14)	1.57 (8)	0.6197 (12)	0.8669 (10)	29.2	1.05	3.83959 (8) × 6 3.633 (3) × 3 4.137 (3) × 3	2.34 (2) 2.282 (5) × 3	2.39 (2) 2.477 (9) × 3
Tb <sup>b</sup>	0.74176 (12)	0.71 (7)	0.6190 (11)	0.8690 (9)	27.5	1.07	3.83966 (6) × 6 3.627 (3) × 3 4.144 (3) × 3	2.35 (2) 2.278 (5) × 3	2.43 (2) 2.462 (8) × 3
Dy	0.74186 (10)	0.40 (5)	0.6185 (10)	0.8729 (9)	24.7	1.08	3.82052 (9) × 6 3.610 (2) × 3 4.117 (2) × 3	2.34 (2) 2.265 (5) × 3	2.48 (2) 2.419 (7) × 3
Ho	0.74187 (6)	1.5 (4)	0.6208 (6)	0.8688 (5)	13.3	1.31	3.80085 (4) × 6 3.591 (2) × 3 4.095 (2) × 2	2.290 (11) 2.263 (3) × 3	2.399 (10) 2.436 (4) × 3
Er	0.74182 (5)	0.95 (3)	0.6194 (5)	0.8684 (5)	11.4	1.20	3.78125 (5) × 6 3.5717 (11) × 3 4.0762 (11) × 3	2.301 (9) 2.246 (2) × 3	2.381 (9) 2.428 (4) × 3

<sup>a</sup>  $B_{iso}$  fixed at 0.7 Å<sup>2</sup>.

<sup>b</sup> TbOF sample heated to 1000 °C for 2 h.

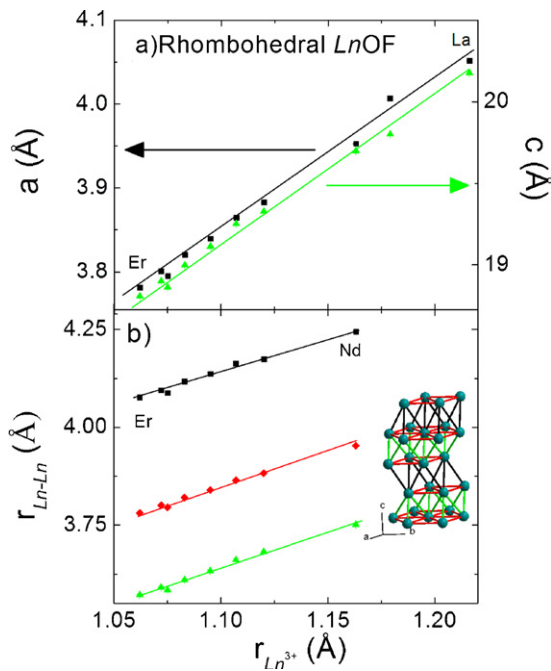


**Fig. 2.** Variation of (a) the lattice parameters and (b) the  $Ln-Ln$  bonds in rhombohedral  $LnOF$  as derived from X-ray diffraction. The  $Ln$  framework in rhombohedral  $LnOF$  is inset, short (green) intermediate (red) and long (black)  $Ln-Ln$  bonds are shown. Lines are a guide to the eye; unless shown error bars are smaller than the data points. (For interpretation of the references to color in this figure legend, the reader is referred to the web version of the article.)

magnetic susceptibility of  $Eu_2O_3$  and  $Eu$ -doped  $Y_2O_3$  has also been attributed to Van Vleck paramagnetism [32–35] and so this is not unexpected for  $Eu^{3+}$  cations. At high temperatures the susceptibility of  $GdOF$  is similar to that of the other  $LnOF$  measured, however at low temperatures a maximum in the susceptibility is observed. We attribute this to the AFM ordering of the  $Gd^{3+}$  cations at  $T_N = 4.0(5)$  K. This transition temperature, though high, is of the correct order for an AFM transition of a  $4f^7$   $Ln^{3+}$  ion. The effective magnetic moment,  $\mu_{eff}$ , and Weiss temperature,  $\theta$ , were obtained from the measured magnetic susceptibilities using the Curie-Weiss law,  $\chi - \chi_0 = C/(T - \theta)$ . To minimize the contribution of CEF effects to the susceptibility, only the low temperature data,  $T < 20$  K, were fit; in the case of  $GdOF$  only data above  $T_N$  were considered. The values obtained are shown in Table 3, for all  $LnOF$  the effective magnetic moments,  $\mu_{eff}$ , are close to the theoretical values and within the range observed in other  $Ln^{3+}$  containing systems. It should be noted that, since the measurements were made on powder samples of  $LnOF$ , the Curie constant and Weiss temperature are powder averaged values; as such any anisotropy in the magnetism cannot be detected [36]. No attempts to fit the Van Vleck paramagnetism of  $EuOF$  have been attempted. In the case of  $NdOF$  and cubic  $PrOF$ , the obtained Weiss temperature is

**Table 3**  
Magnetic characterization of  $LnOF$ .

$Ln$	$\mu_{eff}$ ( $\mu_B$ per fu)	$\theta$ (K)
Pr (cubic)	3.34	<sup>a</sup>
Nd	3.53	<sup>a</sup>
Gd	7.84	-2.4
Tb	9.61	-6.4
Dy	10.56	-6.5
Ho	10.71	-7.8
Er	9.59	-0.08

<sup>a</sup> Significant CEF effects result in a large AFM Weiss temperature; the values obtained have hence been omitted.

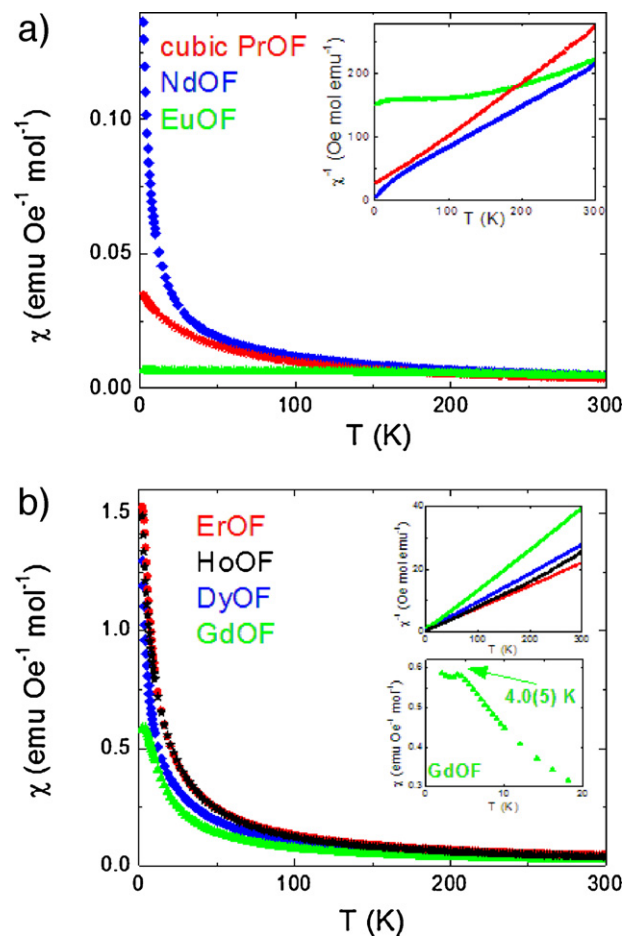


**Fig. 3.** Magnetic susceptibility,  $\chi$ , as a function of temperature for (a) cubic  $PrOF$ ,  $NdOF$  and  $EuOF$  and (b)  $GdOF$ ,  $DyOF$ ,  $HoOF$  and  $ErOF$ . The inverse susceptibility is inset. The antiferromagnetic transition in  $GdOF$  is shown in more detail in the inset of panel (b).

unrealistically high,  $\theta < -20$  K, which we attribute to CEF effects rather than the strength of the true magnetic interactions between  $Ln^{3+}$  ions; these have thus been omitted from the tabulated values. The paramagnetic susceptibility in  $NdOF$  and its relationship to changes in the crystal structure and CEF have previously been discussed in some detail [19,20].

Unlike the other  $LnOF$  studied, the magnetic susceptibility of  $TbOF$  shows evidence for two magnetic transitions; a sharp peak at 10 K and a change in the gradient of the magnetic susceptibility at 5 K (Fig. 4a). At higher temperatures the magnetic susceptibility of  $TbOF$  obeys the Curie-Weiss law with the fitted parameters (Table 3) consistent with those expected for  $Tb^{3+}$  ions. At low temperatures, the sharp transition and the absence of hysteresis between the ZFC and FC susceptibility indicates the presence of long-range three-dimensional ordering,  $T_m = 10$  K. Three-dimensional ordering at such a high temperature is unusual in a  $Ln^{3+}$  magnetic lattice. In  $TbOF$ , this may be due to a significant FM component in the interactions, elevating the ordering temperature. The large spin of the  $Tb^{3+}$ ,  $4f^8$ , cations could also raise  $T_m$ . Isothermal magnetization measurements indicate complex magnetic behavior below the transition(s) (Fig. 4b) with maxima in  $dM/d\mu_0 H$  observed at  $\pm 1.8$  T at both 2 and 8 K (Fig. 4c). At higher fields, the isothermal magnetization below 10 K saturates to  $\sim 7.5 \mu_B$  per Tb, lower than the expected saturation magnetization for  $Tb^{3+}$  of  $8.5 \mu_B$ . The negative Weiss temperature,  $\theta = -6.4$  K and the magnetic susceptibility in 0.1 T suggest that in low fields the magnetic ordering has a dominant AFM component which on application of a

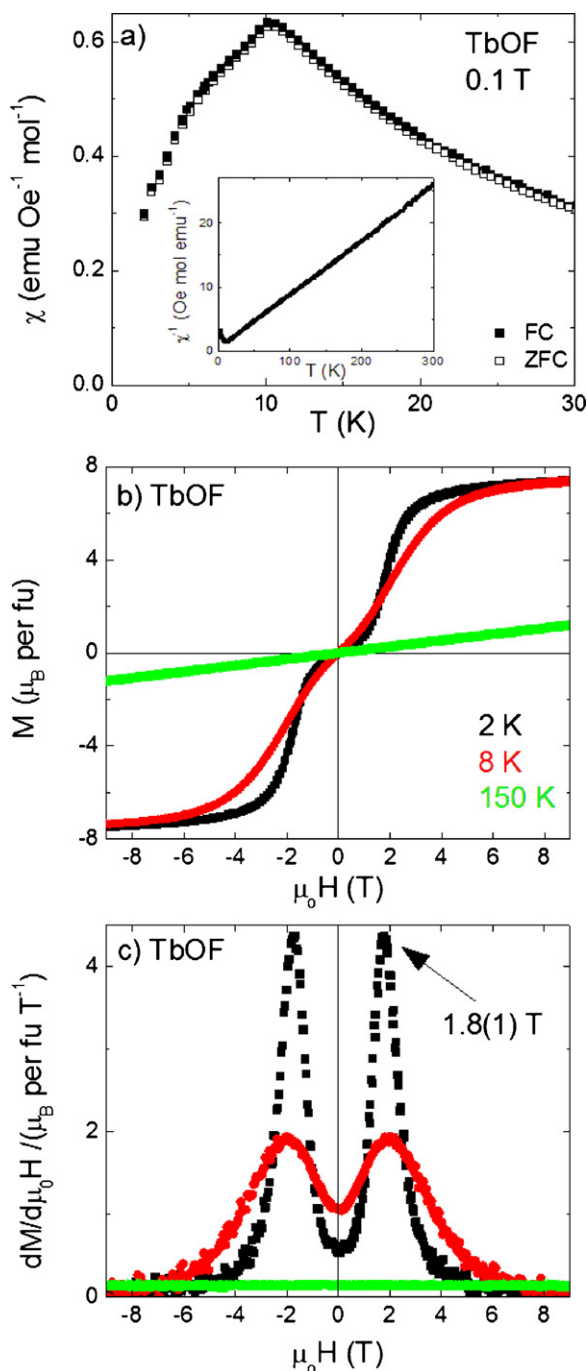


**Fig. 4.** (a) Magnetic susceptibility,  $\chi$ , as a function of temperature for TbOF. Both the ZFC and FC magnetic susceptibility is show, the inverse susceptibility is inset. (b) Isothermal magnetization of TbOF at 2 K, 8 K and 12 K,  $dM/d\mu_0H$  is shown in panel (c).

field undergoes spin-reorientation to a FM-like ordering above 1.8 T [37,38]. Similar behavior has previously been reported in orthorhombic  $TbF_3$ , which orders at 3.95 K [39]. In  $TbF_3$ , the  $Tb^{3+}$ ,  $4f^8$ , ions can be treated as using spins displaying canted AFM order at low fields before undergoing a spin-flip transition at 1.3 T to a canted FM state. Further experiments on single crystals or neutron diffraction

experiments are required to further explore the nature of the magnetic ordering in TbOF.

Our results demonstrate the use of a new solid-state route for the formation of  $LnOF$  by reaction of the rare-earth oxides and PTFE. By tuning the temperature of reaction, we show that  $LnOF$  can be produced for nearly all of the rare-earth elements. Furthermore, unlike other synthetic routes, reaction with PTFE results in the formation of the anion ordered low temperature rhombohedral phase.

#### Acknowledgments

The authors would like to acknowledge helpful discussions with Shuang Jia, Ni Ni, Esteban Climent-Pascual and Collin Broholm. This research was supported by the U.S. Department of Energy, Office of Basic Energy Sciences, Division of Materials Sciences and Engineering under Award DE-FG02-08ER46544.

#### References

- [1] V.I. Klimov, A.A. Mikhailovsky, S. Xu, A. Malko, J.A. Hollingsworth, C.A. Leatherdale, H.J. Eisler, M.G. Bawendi, *Science* 290 (2000) 314–317.
- [2] J.R. O'Connor, *Appl. Phys. Lett.* 9 (1966) 407.
- [3] G. Blasse, A. Bril, *Philips Res. Rep.* 23 (1968) 461.
- [4] W.D. Horrocks, G.F. Schmidt, D.R. Sudnick, C. Kittrell, R.A. Bernheim, *Abstr. Pap. Am. Chem. Soc.* 173 (1977) 36.
- [5] Z.Z. Yu, Q.B. Yang, C.F. Xu, Y.X. Liu, *Mater. Res. Bull.* 44 (2009) 1576–1580.
- [6] S. Shen, A. Jha, *Opt. Mater.* 25 (2004) 321–333.
- [7] Y. Wang, J. Ohwaki, *Appl. Phys. Lett.* 63 (1993) 3268.
- [8] D. Barreca, A. Gasparotto, C. Maragno, E. Tondello, E. Bontempi, L.E. Depero, C. Sada, *Chem. Vap. Deposition* 11 (2005) 426–432.
- [9] Y.-P. Du, Y.-W. Zhang, L.-D. Sun, C.-H. Yan, *J. Phys. Chem. C* 112 (2007) 405–415.
- [10] S. Fujihara, T. Kato, T. Kimura, *J. Mater. Sci. Lett.* 20 (2001) 687–689.
- [11] S. Fujihara, T. Kato, T. Kimura, *J. Sol-Gel Sci. Technol.* 26 (2003) 953–956.
- [12] J. Lee, Q. Zhang, F. Saito, *J. Am. Ceram. Soc.* 84 (2001) 863–865.
- [13] G. Malandrino, L.M.S. Perdicaro, I.L. Fragala, *Chem. Vap. Deposition* 12 (2006) 736–741.
- [14] X. Sun, Y.-W. Zhang, Y.-P. Du, Z.-G. Yan, R. Si, L.-P. You, C.-H. Yan, *Chem. – Eur. J.* 13 (2007) 2320–2332.
- [15] A.P. Ramirez, A. Hayashi, R.J. Cava, R. Siddharthan, B.S. Shastry, *Nature* 399 (1999) 333–335.
- [16] M.J. Harris, S.T. Bramwell, D.F. McMorrow, T. Zeiske, K.W. Godfrey, *Phys. Rev. Lett.* 79 (1997) 2554–2557.
- [17] I. Mirebeau, A. Apetrei, J. Rodriguez Carvajal, P. Bonville, A. Forget, D. Colson, V. Glazkov, J.P. Sanchez, O. Isnard, E. Suard, *Phys. Rev. Lett.* 94 (2005) 246402.
- [18] J.S. Gardner, S.R. Dunsiger, B.D. Gaulin, M.J.P. Gingras, J.E. Greedan, R.F. Kiefl, M.D. Lumsden, W.A. MacFarlane, N.P. Raju, J.E. Sonier, I. Swainson, Z. Tun, *Phys. Rev. Lett.* 82 (1999) 1012–1015.
- [19] L. Beaury, G. Calvarin, J. Derouet, J. Hölsä, E. Säilynoja, *J. Alloys Compd.* 275–277 (1998) 646–650.
- [20] L. Beaury, J. Derouet, J. Hölsä, M. Lastusaari, J. Rodriguez-Carvajal, *Solid State Sci.* 4 (2002) 1039–1043.
- [21] T. Petzel, V. Marx, B. Hormann, *J. Alloys Compd.* 200 (1993) 27–31.
- [22] K. Niihara, S. Yajima, *Bull. Chem. Soc. Jpn.* 44 (1971) 643.
- [23] D.B. Shinn, H.A. Eick, *Inorg. Chem.* 8 (1969) 232–235.
- [24] N.C. Baenziger, J.R. Holden, G.E. Knudson, A.I. Popov, *J. Am. Chem. Soc.* 76 (1954) 4734–4735.
- [25] H.M. Rietveld, *J. Appl. Crystallogr.* 2 (1969) 65–71.
- [26] J. Rodriguez-Carvajal, *Phys. B: Condens. Matter* 192 (1993) 55–69.
- [27] P. Scherrer, *Nachr. Gött.* 2 (1918) 98.
- [28] N.C. Popa, *J. Appl. Crystallogr.* 31 (1998) 176–180.
- [29] N.C. Popa, D. Balzar, *J. Appl. Crystallogr.* 41 (2008) 615–627.
- [30] W.H. Zachariasen, *Acta Crystallogr.* 4 (1951) 231.
- [31] F. Hund, *Z. Anorg. Allg. Chem.* 265 (1951) 62.
- [32] A. Grill, M. Schieber, *Phys. Rev. B* 1 (1970) 2241.
- [33] S. Kern, R. Kosteletzky, *J. Appl. Phys.* 42 (1971) 1773.
- [34] B. Antic, M. Mitric, D. Rodic, *J. Phys.: Condens. Matter* 9 (1997) 365.
- [35] S. Arajas, R.V. Colvin, *J. Appl. Phys.* 35 (1963) 1181.
- [36] E. Morosan, J.A. Fleitman, Q. Huang, J.W. Lynn, Y. Chen, X. Ke, M.L. Dahlberg, P. Schiffer, C.R. Craley, R.J. Cava, *Phys. Rev. B* 77 (2008) 224423.
- [37] L. Holmes, H.J. Guggenheim, G.W. Hull, *Solid State Commun.* 8 (1970) 2005.
- [38] L. Holmes, H.J. Guggenheim, *J. Phys.* 32 (1971) C1 501.
- [39] M. Piotrowski, A. Murasik, *Phys. Status Solidi A-Appl. Res.* 60 (1980) K195–K199.